J Mater Sci (2009) 44:2865–2875
DOI 10.1007/s10853-009-3379-x

Organo-functionalized mesoporous supports for Jacobsen-type catalyst: Laponite versus MCM-41

Pankaj Das · Ana Rosa Silva · Ana P. Carvalho · João Pires · Cristina Freire

Received: 13 November 2008 / Accepted: 2 March 2009 / Published online: 25 March 2009

Abstract In order to exploit the different textural properties of Laponite and MCM-41, specifically in terms of their external versus internal surface areas, in the covalent anchoring of a chiral Mn(III) *salen* complex, these materials were functionalized with 3-aminopropyltriethoxysilane (APTES), subsequently activated with sodium ethoxide, and finally used to anchor the Jacobsen catalyst derivative C1. All the materials were characterized by nitrogen elemental analysis, XPS, PXRD, nitrogen adsorption at −196 °C, FTIR and for those with the immobilized complex, they were additionally characterized by Mn AAS. The APTES anchored at the edges of the Laponite single crystals and inside the MCM-41 pores. Moreover, under the same preparative conditions, higher amount of APTES was anchored onto MCM-41 than onto Laponite, which is due to the higher surface area of MCM-41 compared to Laponite, as well as to its more exposed SiO_4 tetrahedra. Activation of the two organo-functionalized materials with sodium ethoxide originated anionic nitrogen groups as deduced by the increase of surface sodium content of these materials and N1s binding energy changes, but led to a small decrease in N bulk content as a result of some APTES leaching. Moreover, for MCM-41 some disruption of the silica framework occurred as a consequence of the basic treatment, as suggested by XPS, PXRD, and nitrogen adsorption study. The APTES functionalized Laponite and MCM-41 materials, as well as the activated analogs, were able to anchor C1 through axial coordination of the metal centre to the grafted surface nitrogen atoms. APTES functionalized MCM-41 presented similar complex content to Laponite analog, what points out for the fact that, at least for the bulky complex used in this work, there was no clear benefit in using a material of high internal area; for the ethoxide activated analogs, Laponite showed the highest complex content of all materials, but MCM-41 was able to anchor the lowest complex quantity, probably as a consequence of damaging effect caused by the basic treatment within its porous structure.

Electronic supplementary material The online version of this article (doi:10.1007/s10853-009-3379-x) contains supplementary material, which is available to authorized users.

P. Das · A. R. Silva · C. Freire (✉)
REQUIMTE, Departamento de Química, Faculdade de Ciências, Universidade do Porto, Rua do Campo Alegre, 4169-007 Porto, Portugal
e-mail: acfreire@fc.up.pt

A. P. Carvalho · J. Pires (✉)
Departamento de Química e Bioquímica and CQB, Faculdade de Ciências, Universidade de Lisboa, Ed. C8, Campo Grande, 1749-016 Lisbon, Portugal
e-mail: jpsilva@fc.ul.pt

Present Address:
P. Das
Department of Chemistry, Dibrugarh University, Dibrugarh, Assam 786 004, India

Present Address:
A. R. Silva
Unilever R&D, Port Sunlight, Bebington, UK

Introduction

Jacobsen-type catalysts are excellent homogeneous catalysts for the asymmetric epoxidation of alkenes, which is a powerful strategy for the synthesis of chiral intermediates in the pharmaceutical, as well as agrochemical industries [1–3]. To get a heterogeneous system with easy separation and better handling properties than the homogeneous

system, as well as with potential reusability, several attempts have been made to immobilize Jacobsen-type catalysts into or onto different supports. These attempts include grafting the catalyst onto silica [4, 5], MCM-41 [6–14], encapsulation into the pores of zeolite [15–17], polymer support [18–22], clays [23–25], activated carbon [26–28], etc. Much of the work has been focused on tethering or covalently anchor the homogeneous complexes onto insoluble inorganic supports with the aid of organosilane coupling reagents [7, 9–14, 29–33], in order to keep the catalyst active centre away from the support material so that it apparently behaves like an homogeneous catalyst. Surface covalent anchoring of the complex through the ligand is one of the most used methods for complex immobilization [7, 19–22]. However, these procedures often require complicated synthetic manipulations and structure modification of the ligands, which ultimately result in low activities and enantioselectivities. Lately, there have been several reports on the anchoring of Mn(III) *salen* complex through the metal centre to the functionalized surface, which has been proving to be a very effective and easy way to obtain efficient and reusable heterogeneous catalysts [9–11, 13, 27, 28, 31].

Laponite is a synthetic material similar to the smectite type clays (but the octahedral aluminum was substituted by magnesium) and belongs to the family of so called swelling 2:1 clays. Additionally, it has regular crystallites of small size (in the range of the several nm). It is a low cost synthetic material possessing reactive surface Si–OH group, which are mostly located at the edge of the clay sheets [34]. Its high ratio of edge to surface area makes it an ideal candidate for edge surface modification by using some organic functionalities (spacers) possessing reactive groups, like amine ($–NH_2$), which permits immobilization of metal complexes through coordinative bond with the metal centre. In fact, there are some reports [34–38] on modification of edge surface of Laponite by using alkoxysilane possessing an additional reactive functionalities, but to the best of our knowledge, besides our recent reports [38–40] on the immobilization of a non-chiral complexes onto Laponite through three different immobilization procedures, there are no further reports of immobilization of transition metal complexes by using surface edge modified Laponite. On the other hand, there are some reports on the covalent attachment of Mn(III) *salen* complexes onto organosilane modified MCM-41 [7–14]; this is a mesoporous material with large surface area possessing surface reactive Si–OH group, but which are mostly located at the interior wall of the mesoporous channels unlike the Laponite [29, 41, 42].

The comparison, in terms of costs of the preparation of Laponite and MCM-41 is not straightforward. In fact, in the future MCM-41 can also find other type of applications and can eventually be prepared in large amounts worldwide, thus making it cheaper. Presently, Laponite, for a commercial material, is not much expensive since it is produced in large amounts and finds applications in fields, such as surface coatings, agricultural, building products, personal care products, and household products.

In the present work Laponite and MCM-41 were functionalized with 3-aminopropyltriethxysilane (APTES) and both NH_2-functionalized materials were also activated by sodium ethoxide; with this step we attempt to create new anionic nitrogen grafted species with high donor property for metal coordination. All the organo-functionalized supports were used to covalently anchor the Jacobsen catalyst derivative (C1). In parallel, we endeavor to exploit the different textural properties of these two materials (Laponite vs MCM-41) that is, external versus internal surface area materials, in the anchoring of chiral Mn(III) *salen*-type complexes. In fact, and in spite of the large number of studies published in the literature concerning the immobilization of Jacobsen-type catalysts in various types of supports, the question wherever the most favorable supports are high external or internal (porous) area materials is still not well defined. Our ultimate goal is the preparation of stable and recyclable catalysts for the asymmetric epoxidation of alkenes; the catalytic properties of these materials are being published elsewhere, jointly with the results from the same complex immobilized in FSM-16 [43, 44].

Experimental

Parent materials, solvents, and reagents

Tetraethoxysilane, cetyltrimethylammonium bromide, (*R,R*)-(−)-*N,N′*-Bis(3,5-di-*tert*-butylsalicylidene)-1,2-cyclohexanediaminomanganese(III) chloride (Jacobsen catalyst-(*R,R*)-[Mn(3,5-dtButsalhd)Cl]), silver perchlorate, 3-aminopropyltriethoxysilane (APTES), sodium ethoxide solution (NaOEt, 21%) in ethanol were purchased from Aldrich. Aqueous ammonia and all the solvents used were purchased from Merck (*pro analysis*).

Laponite was obtained from Laporte Industries Ltd. (UK) and was used as received. Its structural formula, as indicated by the supplier, is $Na_{0.7}[(Si_8Mg_{5.5}Li_{0.3})O_{20}(OH)_4]$; the powder X-ray diffraction (PXRD) is presented in Fig. S1 in Supplementary Material. MCM-41 was synthesized according to procedures described in the literature [45, 46]. Briefly, cetyltrimethylammonium bromide was dissolved in deionized water and aqueous ammonia; the silica source was the tetraethoxysilane. The solid was dried at 90 °C and heated under air at 550 °CC for 5 h, after a ramp of 1 °C min^{-1} for removing the organic moieties. From the results of PXRD the peaks corresponding to d_{100}, d_{110}, and d_{200} were noticed at values of 3.78, 2.17, and 1.91 nm,

respectively, within the range of published values [45, 46], Fig. S2 in Supplementary Material. The a_0 parameter of the prepared sample, considering a hexagonal symmetry, is 4.37 nm.

Preparation of materials

Modification of supporting materials

Anchoring of APTES onto Laponite and MCM-41 Laponite and MCM-41 were functionalized with APTES by following a method described in the literature [32]. In the present case, 1.5 g of Laponite (L1) or MCM-41 (M1) were refluxed for 24 h with 0.9 cm^3 (3.8 mmol) of APTES in 100 cm^3 in dry toluene, under nitrogen atmosphere. After cooling, the solids were filtered, Soxhlet extracted with toluene for 24 h and then dried at 120 °C, under vacuum, overnight. The functionalized materials were designated as L2 (for Laponite) and M2 (for MCM-41).

Activation of APTES functionalized Laponite and MCM-41 1.0 g of L2 and M2 was refluxed for 4 h with 1.25 cm^3 (3.86 mmol) of a solution 21% in sodium ethoxide in ethanol. After filtering the solid materials they were Soxhlet extracted with ethanol for 24 h and then dried at 120 °C, under vacuum, overnight. The functionalized materials were designated as L4 (for Laponite) and M4 (for MCM-41).

Immobilization of C1

The commercial Jacobsen catalyst (0.05 g, 80 mmol) was dissolved in 50 cm^3 of acetonitrile, and to this solution 0.02 g (95 mmol) of $AgClO_4$ were added. The solution was stirred for 4 h at room temperature. After filtration of silver chloride and solvent removal, a reddish brown complex (*R*,*R*)-[Mn(3,5-dtButsalhd)]ClO_4 (C1) was obtained.

C1 anchoring onto the functionalized Laponite and MCM-41 A solution of complex (C1) (80 mg; 114 μmol) in 100 cm^3 of dichloromethane was refluxed for 4 h, and then left stirring overnight, with 1.0 g of L2, M2, L4, or M4. After cooling, the solid materials were filtered Soxhlet extracted with dichloromethane for 24 h and then dried at 120 °C, under vacuum, overnight to get the immobilized catalysts. The materials were designated as L3, M3, L5, or M5, respectively (where L refers to the Laponite-based materials and M to the MCM-41 based materials).

The summary of the methodologies used in the organofunctionalization of Laponite and MCM-41 materials and subsequent C1 anchoring are presented in Scheme 1.

Characterization methods

Nitrogen contents were obtained by elemental analysis at 'Laboratório de Análises', IST, Lisboa (Portugal). The bulk Mn content was determined by Atomic Absorption Spectroscopy (AAS) in a Pye Unicam SP9 spectrometer. Typically one sample of 20 mg of solid, previously dried at 100 °C, was mixed with 2 cm^3 of aqua regia and 3 cm^3 of HF for 2 h at 120 °C, in a stainless steel autoclave equipped with a polyethylene-covered beaker (ILC B240). After reaching room temperature the solution was mixed with about 2 g of boric acid and finally adjusted to a known volume with deionized water.

Nitrogen adsorption isotherms at −196 °C were measured in an automatic apparatus (Asap 2010; Micromeritics). Before the adsorption experiments, the samples were outgassed under vacuum during 2.5 h at 150 °C. Microporosity, as evaluated from the *t*-method [47], was not present on any of the studied materials. The mesoporous volumes were obtained from the amounts adsorbed at high relative pressures ($p/p^0 \sim 0.97$), and specific surface areas were obtained by the BET method [47].

Powder X-ray diffractograms were obtained in Philips PX 1730 diffractometer using Cu Kα radiation, with a step size of 0.005 ($2\theta^\circ$) and a time per step of 2.5 s.

FTIR spectra of the materials were obtained as KBr pellets (Merck, spectroscopic grade) in the range 400–4000 cm^{-1}, with a Jasco FT/IR-460 Plus spectrophotometer; all spectra were collected at room temperature, after drying the pellets in an oven overnight, using a resolution of 4 cm^{-1} and 32 scans.

X-ray photoelectron spectroscopy was performed at "Centro de Materiais da Universidade do Porto" (Portugal), in a VG Scientific ESCALAB 200A spectrometer using a non-monochromatised Mg Kα radiation (1253.6 eV). All the materials were compressed into pellets prior to the XPS studies. In order to correct possible deviations caused by electric charge of the samples, the C 1 s line at 285.0 eV was taken as internal standard. The elemental contents of the various samples were calculated from the areas of the relevant bands in the high resolution XPS spectra, which were also curve fitted using symmetric Gaussian curves, after fitting to a Shirley background, using XPS peak version 4.1.

Results and discussion

Modification of Laponite and MCM-41 surface

Chemical analysis

Analysis of bulk N contents in Table 1 shows that APTES anchoring onto Laponite (L2) is less than in MCM-41 (M2), which indirectly implies that MCM-41 contains more surface reactive hydroxyl groups than Laponite, a situation that is most probably related with

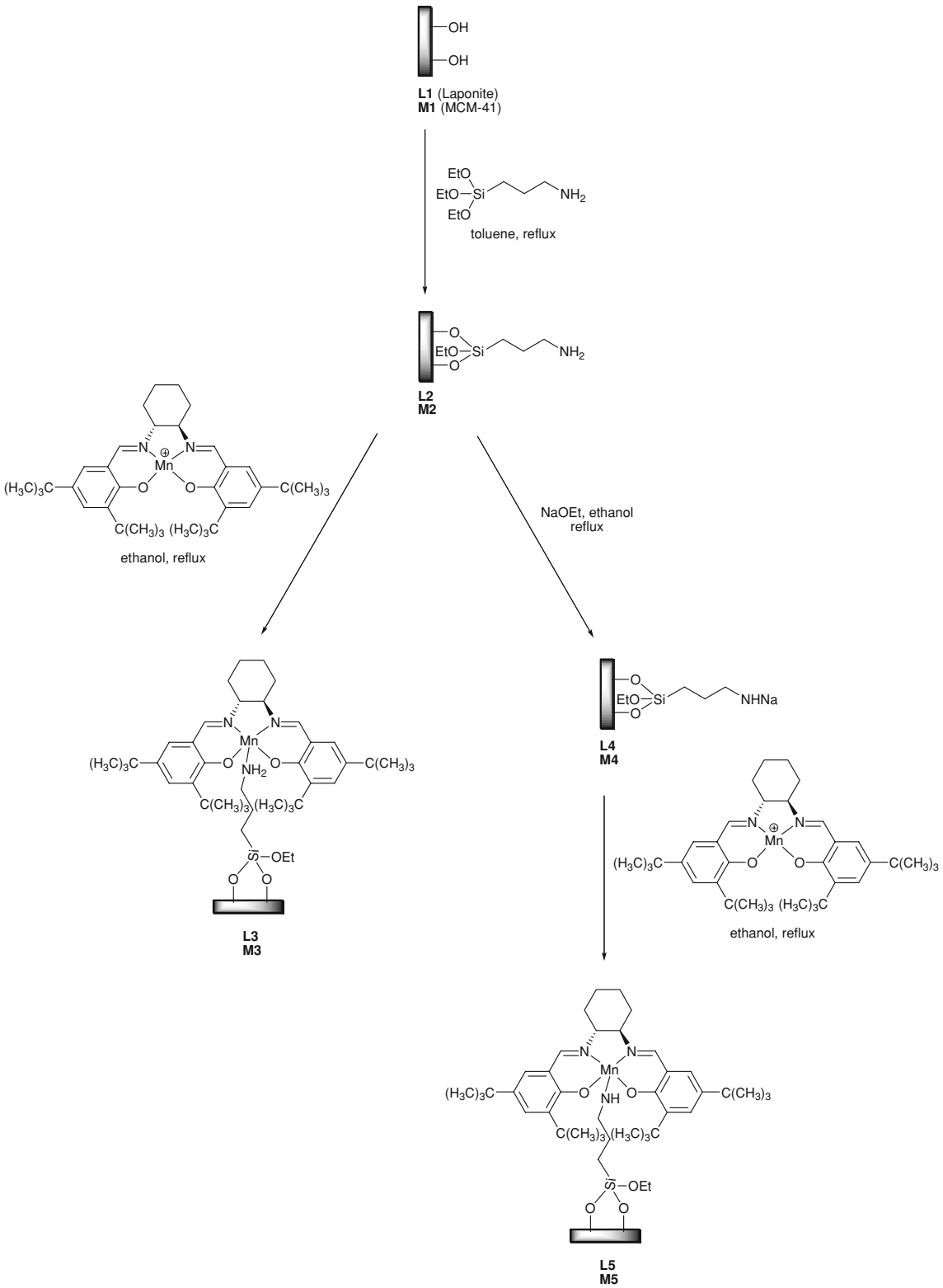

Scheme 1 Immobilization methodologies used in the immobilization of C1 onto organo-functionalized Laponite and MCM-41 materials

the higher surface area of the MCM-41 material and also to the different arrangements of the SiO_4 tetrahedra in each material.

It is noteworthy that higher amounts of linked APTES to Laponite were obtained herein than on the report of Wheeler et al. [34] on the edge-covalent functionalization of Laponite

Table 1 Nitrogen and manganese contents determined from elemental analysis and XPS and textural properties of the Laponite and MCM-41 base materials

Materials	N (mmol g^{-1})		Mn (μmol g^{-1})		Textural properties[d]	
	EA[a]	XPS[b]	AAS[c]	XPS[b]	A_{BET} (m^2/g)	V_{meso} (cm^3/g)
L1	–	–	–	–	378	0.25
L2	1.1	1.56	–	–	122	0.13
L3	1.3	1.56	7.5	70	48	0.06
L4	0.51	0.45	–	–	n.d.	n.d.
L5	0.51	0.64	16.0	26	73	0.04
M1	–	–	–	–	1087	0.86
M2	1.8	1.20	–	–	734	0.39
M3	1.7	1.21	8.0	168	340	0.21
M4	1.5	1.38	–	–	20	–
M5	1.6	1.35	1.2	21	5	–

[a] *EA* nitrogen elemental analysis

[b] N or Mn amount per weight of sample calculated from XPS data in Table 2: mmol N or Mn/weight of sample = at.% N or Mn/[at.% C × Ar(C) + at.% N × Ar(N) + at.% O × Ar(O) + at.% Mg × Ar(Mg) + at.% Si × Ar(Si) + at.% Cl × Ar(Cl) + at.% Mn × Ar(Mn) + at.% Na × Ar(Na)]

[c] *AAS* atomic absorption spectroscopy

[d] From the nitrogen adsorption isotherms at −196 °C

with a similar organosilane, 3-aminopropyltrimethoxysilane (APTMS), under several experimental conditions, in which they were able to obtain by TGA analysis 4.2–12.6% of organic content, which corresponds to 0.25–0.70 mmol of 3-aminopropyltriethoxysilane per g of material.

Upon NaOEt treatment of the amine-functionalized materials a decrease in nitrogen is observed (L4 and M4) which may be a result of leaching of some of the anchored APTES, probably due to some hydrolysis of –O–Si–$(CH_2)_3NH_2$ bonds under the alkaline conditions of the media. It is worth mentioning that the nitrogen decrease is slightly higher for L2 than for M2.

It should be emphasized at this point that, because the APTES molecules are hydrolytically very unstable, its pKa value can not be evaluated directly. In this way, its pKa value is normally approached by the value of the propylamine which is 10.6 [48, 49]. Considering the pKa of the ethanol as 15.9 [50] it can be found that the deprotonation of APTES by ethoxide is highly favored since the equilibrium constant is about $10^{5.3}$. On the basis of this constant and the amounts of APTES and sodium ethoxide given in the experimental part it is expected that more than 70% of APTES will be deprotonated in the formation of L4 and M4.

XPS

The chemical composition obtained by XPS for the Laponite and MCM-41 based materials are collected in Table 2

Table 2 XPS data (at.%) of the Laponite and MCM-41 base materials

Materials	C	N	O	Na	Mg	Si	Cl	Mn
L1	13.18	–	50.53	2.22	13.51	20.56	–	–
L2	21.46	2.88	44.48	1.72	9.00	20.06	0.40	–
L3	18.53	2.91	47.05	2.04	8.51	20.39	0.44	0.13
L4	17.00	0.86	46.12	3.84	11.21	20.58	0.39	–
L5	14.20	1.23	47.91	3.27	11.81	20.94	0.58	0.05
M1	15.59	1.48	53.11	–	–	29.82	–	–
M2	19.01	2.22	50.73	–	–	27.94	0.10	–
M3	18.46	2.30	48.50	–	–	30.01	0.40	0.32
M4	17.32	2.60	48.33	6.91		23.75	1.08	–
M5	18.23	2.53	48.05	6.37	–	23.60	1.18	0.04

and the results of the deconvolution of the high resolution spectra are collected in Table S1, in Supplementary Material—Curve fitting data of the XPS spectra in the relevant regions of the Laponite and MCM-41 based materials.

The high resolution XPS spectra of parent Laponite (L1) shows the following bands: (i) in the Si 2p region at about 103.0 eV, which corresponds to silicon from the tetrahedral sheets of the clay; (ii) a symmetrical band at 532.0 eV in the O 1s region, due to single bonded oxygen from silica lattice; (iii) a band centered at 1304.0 eV in the Mg 1s region, due to the Mg^{2+} cations present in the octahedral sheets; (iv) a band centered at 1072.6 eV in the Na 1s region, due to the exchangeable Na^+ cations within the interlayers. The parent MCM-41 material (M1) shows bands in the Si 2p region at about 104.5 eV, which corresponds to the SiO_4 framework of the material and a symmetrical band at 533.8 eV in the O 1s region, due to single bonded oxygen from silica lattice. Low intense and broad bands at the C 1s region and N 1s are also observed for both materials which are due to the presence of some organic impurities resulting from the synthesis of the materials (Table 2 and Table S1). It is remarkable that the binding energies of the Si 2p and O 1s bands are higher in energy in the case of MCM-41 than for Laponite, suggesting that both elements are more electron de-protected in MCM-41. This may be attributed to differences in the structure of both materials.

Upon surface functionalization with APTES of both materials (L2 and M2) it can also be seen that there is an increase of surface carbon content in addition to the increase in nitrogen content due to the anchoring of the spacer. For Laponite, higher surface content of nitrogen was obtained by XPS than by bulk analysis (Table 1), indicating that the APTES linker is mostly located at the external surface of the material. For MCM-41 the opposite is observed: lower surface content of nitrogen compared to bulk nitrogen elemental analysis (Table 1), indicating that

the APTES is mostly located in the internal pore structure of the material. These results correlate well with the location of the reactive hydroxyl groups on these materials.

Reflux of the amine-functionalized Laponite and MCM-41 materials with NaOEt (L4 and M4) results in a significant increase in the surface sodium content of both materials and a change in the nitrogen binding energy (Table S1); this suggests the formation of new anionic nitrogen species at the surface of both materials. Furthermore, Laponite also shows a decrease in the surface nitrogen content due to partial leaching of the APTES spacer.

It is interesting to note that for M4 a new small band at 536.4 eV in the Si 2p high resolution spectra is observed, in addition to the usual intense and symmetric band at 532.5 eV, Table S1; this result suggests the presence of new silicon species on the surface material and lead us to check the integrity of the material by PXRD. The absence of the typical PXRD peaks of MCM-41 (Fig. S3 in Supplementary Material), suggest that some disruption of the silica framework as a consequence of the NaOEt treatment.

Nitrogen adsorption at −196 °C

The nitrogen adsorption–desorption isotherms for all materials are presented, respectively, in Fig. 1a, b, and the corresponding values of equivalent surface area (A_{BET}) and mesoporous volumes are given in Table 1. It can be seen from Fig. 1 that both materials present characteristics that are related with the presence of mesopores [47]. In fact, the nitrogen isotherms, particularly in the case of the parent solids, and also in the solids with APTES, are of Type IV according to the IUPAC classification [51], although in the case of the MCM-41 samples the isotherms do not present a hysteresis loop and are therefore classified of Type IVc. Nitrogen adsorption isotherms of Type IVc were reported also by other authors for MCM-41 for samples with low mesopores sizes [45, 46], and reflect the existence of uniform near-cylindrical pores [47]. Concerning the origin of the mesoporosity, in the MCM-41 the mesoporores are in the internal porous structure of the material, whereas in the Laponite the mesoporosity results from the aggregation of the single crystals of this solid, as discussed in a previous work [38]. It can also be seen from Table 1 that the MCM-41 has almost 3 times more surface area (A_{BET}) than Laponite and almost 4 times more mesoporous volume.

Upon surface functionalization with APTES (L2 and M2), Scheme 1, there is a decrease in the surface area to about 30% and 70% of the initial values for Laponite and MCM-41, respectively. The mesoporous nature of the MCM-41 is kept after the reaction with APTES, since no microporosity was detected by the *t*-method analysis, although the total mesoporous volume available was considerably reduced.

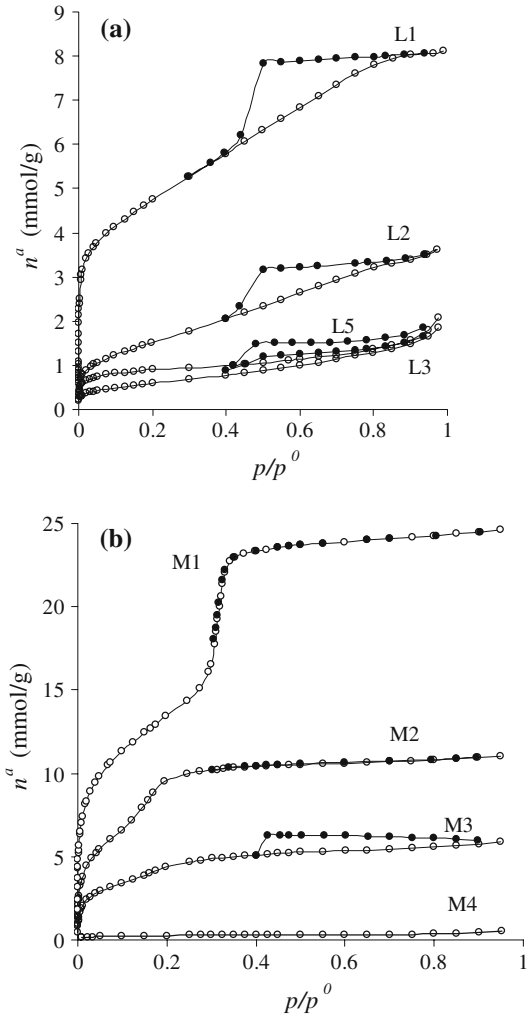

Fig. 1 Nitrogen adsorption–desorption isotherms at −196 °C of **a** Laponite and **b** MCM-41 based materials. Open points for adsorption and closed points for desorption

Activation of the APTES functionalized MCM-41 (M4), Scheme 1, lead to a quite significant decrease in the A_{BET} values, a consequence of the mesoporous structure collapse, as clearly seen from the N_2 isotherm profile shown in Fig. 1b, and confirmed by the XPS and PXRD data. No results could be obtained for the Laponite analog (L4), due to lack of sample quantity. Nevertheless, the results obtained for L5 (material with the anchored complex) indicate no significant changes in the N_2 isotherm profile, anticipating a similar behavior for L4 sample.

In the case of MCM-41 materials, the mesoporosity was further characterized by analyzing the adsorption branch of the nitrogen adsorption isotherms by the Broekhoff-de Boer method, in a version simplified by the use of the Frenkel–Halsey–Hill equation (BdB-FHH method) [52, 53] and the results of the pore size distributions so obtained are shown in Fig. 2. It can be seen from Fig. 2 that for the parent MCM-41 material the maximum in the distributions occurs for a value

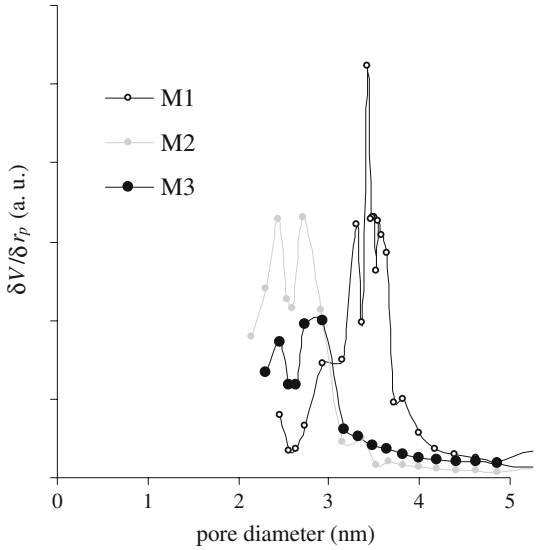

Fig. 2 Mesopore distribution obtained by the BdB-FHH method for the MCM-41 based materials

of 3.4 nm. This value is near the 3.37 nm value that is obtained for the pore diameter from the X-ray data, using the a_0 value given in the experimental part (4.37 nm) if, in a first approximation, the silica walls are considered uniform with a thickness of 1.0 nm [45, 46]. For the sample with APTES (M2) the maxima is shifted to 2.4–2.7 nm, i.e. the space available in the mesopores was reduced by 1–0.7 nm. This decrease is consistent with literature values for MCM-41 materials after a high degree of silylation [54], and was maintained after the linkage of the complex.

FTIR

The FTIR spectra of the series of Laponite-based materials (L1, L2, and L4) and MCM-41-based materials (M1, M2, and M4) are collected, respectively in Fig. 3 and 4.

The spectrum of L1 and M1 exhibit two bands due to the presence of physisorbed water, namely the O–H stretching frequency at 3460 cm^{-1} (L1) and 3420 cm^{-1} (M1), [10, 55] and the O–H deformation band at 1634 cm^{-1} (L1) and 1631 cm^{-1}(M1). For L1, there is also a band at 3683 cm^{-1} due to surface hydroxyls, which presumably consists of the overlapping of two components at 3675 and 3686 cm^{-1} corresponding, respectively, to Si–OH and Mg–OH stretching vibrations [35, 38]; for M1 a shoulder at 3740 cm^{-1} due to isolated surface silanol groups is also observed [54].

L1 and M1 spectra are dominated by the bands associated with SiO_4 framework vibrations. For L1 there is one broad band with peak maximum at 1010 cm^{-1} assigned to transverse and longitudinal Si–O–Si asymmetric stretching vibrations [56], one band at 550 cm^{-1} to Mg–O vibration [35, 38], and a strong band at about 460 cm^{-1} due to SiO_4

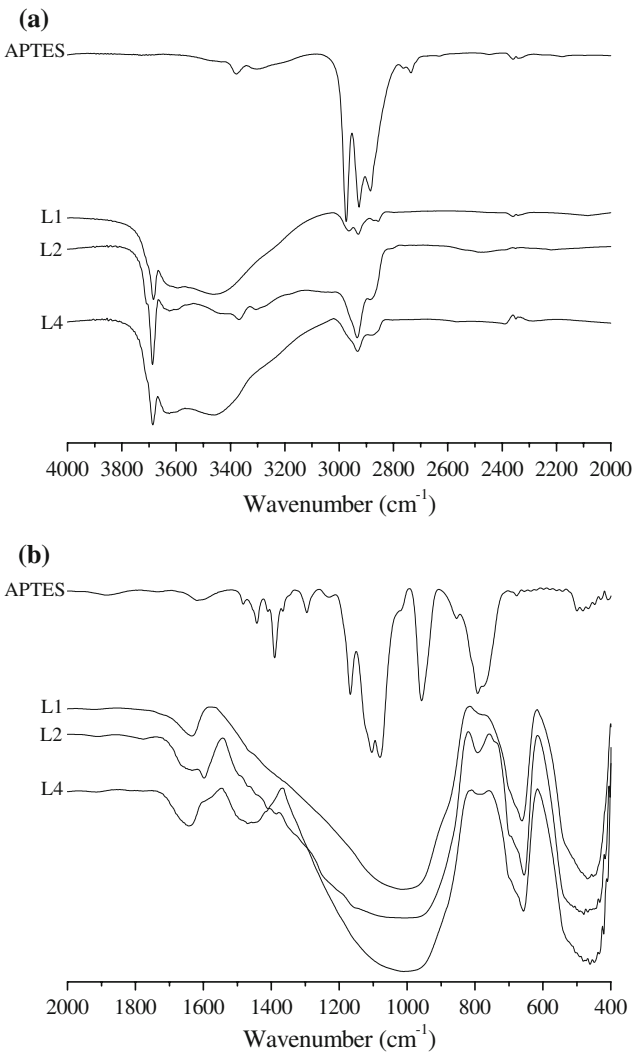

Fig. 3 FTIR spectra of the Laponite-based materials in the **a** 4000–2000 cm^{-1} and **b** 2000–400 cm^{-1} regions

bending vibrations [57]. M1 shows a very intense and large band at about 1080 cm^{-1} due to Si–O–Si linkage of SiO_4 tetrahedra [57], transverse and longitudinal asymmetric network motions, a strong band at around 960 cm^{-1} for the presence of Si–OH stretching vibrations [56, 58], at 800 cm^{-1} for the not resolved transverse and longitudinal symmetric network motions of the SiO_4 tetrahedra [56], and a strong band at about 460 cm^{-1} due to SiO_4 bending vibrations [57].

Upon functionalization of L1 and M1 with APTES (L2 and M2), Scheme 1, several changes are observed: for M2 the broad band around 3420 cm^{-1} becomes sharper and shifted to higher energies and the shoulder at 3740 cm^{-1} due to isolated surface silanol groups disappear [52, 54], whereas for L2 the intensity of the broad band around 3460 cm^{-1} decrease and the band due to the surface hydroxyl groups becomes sharper and shifts to 3686 cm^{-1}

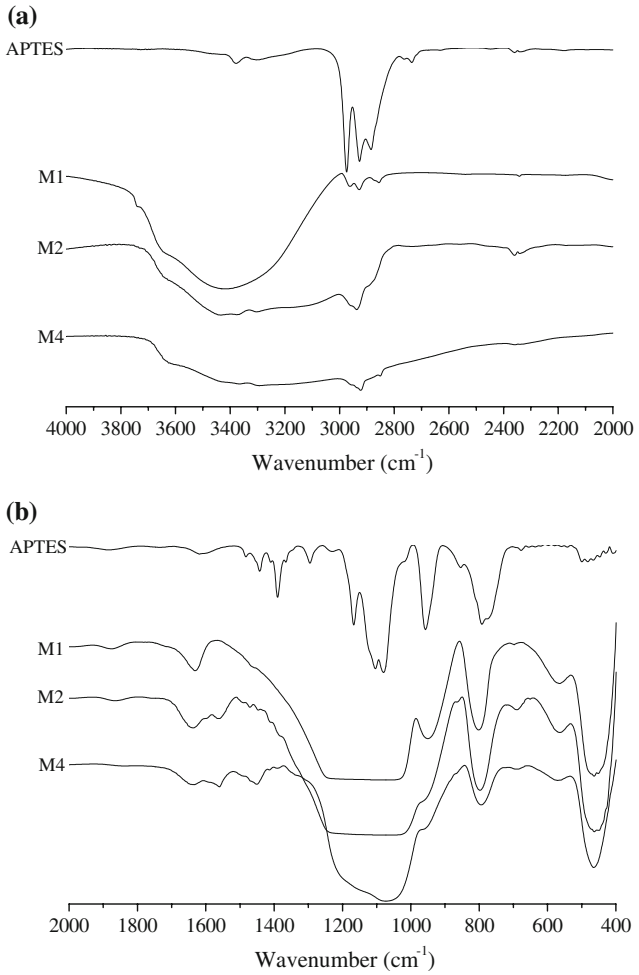

Fig. 4 FTIR spectra of MCM-41 based materials in the **a** 4000–2000 cm^{-1} and **b** 2000–400 cm^{-1} regions

(the Mg–OH stretching vibration) [35, 38]. In addition, L2 and M2 also show two broad bands at 3369 and 3307 cm^{-1} (L2) and 3377 and 3303 cm^{-1} (M2) due to N–H asymmetric and symmetric stretching vibrations, respectively; sharp bands between 2940–2870 cm^{-1} typical of C–H stretching vibrations; a band at 1599 cm^{-1} (L2) and 1563 cm^{-1} (M2) due to N–H scissoring (bending); several bands between 1400 and 1500 cm^{-1} due to C–H bending and C–N stretching [57]; and one band at 793 cm^{-1} (L2) due to the linker molecule. It is noteworthy that the presence of residual Mg–OH groups in Laponite after grafting indicates that these groups are not accessible to the APTES molecule, as expected from their location in the clay structure [35]; moreover, the relative increase in Mg–OH band intensity is due to decrease in physisorbed water after grafting of APTES [35, 38], which is also promoted by the intensity decrease of the hydrogen-bonded hydroxyls stretching vibrations (3460 cm^{-1}) [35]. All the observed changes prove that APTES was covalently attached onto the Laponite edges and MCM-41 surface silanol groups.

After reflux of the APTES functionalized Laponite and MCM-41 materials with NaOEt (L4 and M4) several changes in the respective spectra were detected (Fig. 3 and 4): for L4 the band at 1599 cm^{-1}, due to N–H scissoring (bending) decreases in intensity, a new large band centred at 1460 cm^{-1} appears and the band at about 3460 cm^{-1} becomes more intense and large. For M4 the band due to N–H scissoring (bending) becomes sharper and shifted to 1560 cm^{-1} and changes in the intensities of the C–H bending bands between 1400 and 1500 cm^{-1} are observed, being the one at 1450 cm^{-1} the most intense and evident. These observations, as before, suggest that the surface amine groups of both materials were also modified after the reaction with NaOEt.

Complex immobilization

Chemical analysis

The chiral complex, C1, was synthesized by exchanging the coordinated chloride anion from the Jacobsen's complex with ClO_4^- (a non coordinating anion), in order to promote the immobilization the complex onto Laponite and MCM-41 through metal axial coordination to the nitrogen grafted species following the strategies shown in Scheme 1. On the basis of the Mn AAS data, the amount of complex immobilized onto L3 is similar to that of M3 (7.5–8.0 μmol g^{-1}, respectively) indicating that under the same preparative conditions, comparable amounts of complex were anchored onto MCM-41 and Laponite, despite of the higher content of free amine groups in the MCM-41 material (vide supra).

As determined by AAS, Table 1, L5 is able to anchor a double amount of complex 1 (16.0 μmol g^{-1}) compared to the non-activated analog (L3), whereas the NaOEt refluxed amine-functionalized MCM-41, M5, a low amount of Mn(III) was immobilized (1.2 μmol g^{-1}). This latter result is probably due to the partial collapse of the MCM-41 mesoporosity referred above.

XPS

Upon complex anchoring in both L2 and M2 materials there is an increase in Mn and Cl surface contents (Table 2). Nevertheless, the Mn values obtained by XPS are higher than those obtained by AAS (Table 1), suggesting that the complex has been mostly anchored at the surface of both materials. Furthermore, for both materials a change in the N binding energy is observed, which suggests that the Mn(III) *salen* complex anchored axially through this group.

Similarly, the complex anchoring onto both sodium ethoxide refluxed materials, L4 and M4, leads to an

increase in Mn and Cl surface contents (Table 2). This is accompanied by a decrease in the Na surface content, indirectly showing that the complex is axially anchored onto the new anionic nitrogen species, by elimination of the sodium cation. The Mn values obtained by XPS are higher than those obtained by AAS (Table 1), but are of the same order of magnitude of L5, suggesting once more, that the complex is anchored more externally within the material porous structure.

Nitrogen adsorption at −196 °C

It is useful at this point to discuss separately the case of Laponite and the case of MCM-41. For Laponite, in the L3 and L5 samples there is a surface area decrease, which can be due to the fact that the complex can promote some degree of separation of the clay layers and/or a different arrangement of the crystallites, but the general shape of the isotherm is maintained. In the case of the MCM-41 material, the complex anchoring using APTES (M3) has considerably different effects in the textural properties when comparing with the anchoring after activation with sodium ethoxide (M5). In fact, M3 shows a reduction in the surface area to about 50%, when compared to M2, presents hysteresis (Fig. 1b) that is probably related to changes in the mesoporosity due to the attachment of the bulky complex more externally, (as confirmed by surface vs bulk Mn contents), *c.a.* at the entrance the pores, but the maximum in the pore size distribution was not significantly changed (cf. Fig. 2). The reduction in the surface of M5 is quite drastic when compared with the initial material M1, but predictable if we consider that C1 was anchored in M4, which we showed by XPS and PXRD that disruption of the silica framework has occurred as a consequence of the activation of the free amine groups with NaOEt.

FTIR

The FTIR of the immobilized chiral Mn(III) *salen* complex onto nitrogen-functionalized Laponites and MCM-41 materials (L3, L5, and M3, M5) show small changes compared to the respective parent materials; in Fig. 5, the FTIR spectra of the free and immobilized chiral Mn(III) *salen* complex onto the nitrogen-functionalized Laponites, L3 and L5, are shown.

In L3 spectrum there are not significant changes relatively to the parent material, except for a new band at 1634 cm^{-1}. Similarly, in L5 there are no significant changes, but only a decrease in intensity of the band at 1599 cm^{-1}, due to N–H scissoring (bending), and a shift to lower energies of the large band centered at 1460 cm^{-1}, probably due to C–N stretching are observed; the same type of changes are observed for the analogues MCM-41

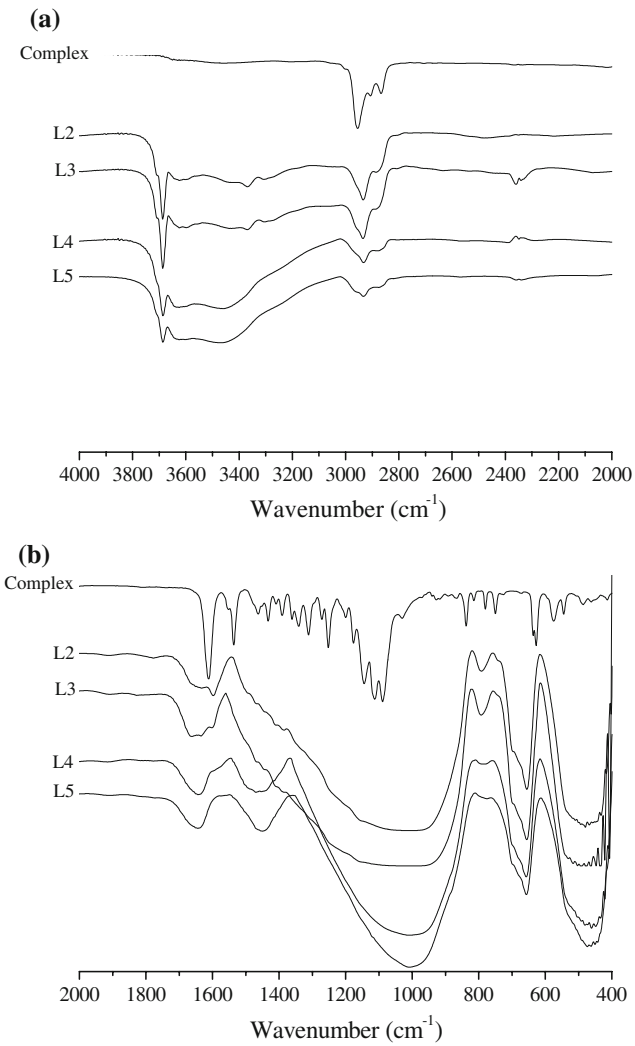

Fig. 5 FTIR spectra of Laponite-based materials and with immobilized Jacobsen catalyst derivative in **a** 4000–2000 cm^{-1} and **b** 2000–400 cm^{-1} regions

based materials. In this way, Mn(III) *salen* anchoring in Laponite and MCM-41 based materials, leads to spectral changes associated with bands due to the grafted spacer, confirming its key role in complex immobilization.

Conclusions

The Jacobsen catalyst derivative C1, was immobilized onto two types of mesoporous materials, Laponite and MCM-41, possessing different textural properties (external vs internal surface area), after functionalization with 3-aminopropyltriethoxysilane (APTES) and activation of the APTES surface modified materials with sodium ethoxide.

Characterization of APTES-grafted Laponite and MCM-41 materials by nitrogen elemental analysis, XPS, FTIR, and nitrogen adsorption at −196 °C showed that the linker

was anchored at the edges of the Laponite single crystals and inside the MCM-41 pores. Moreover, under the same preparative conditions, higher amount of APTES was anchored onto MCM-41 than onto the Laponite, which is due to the higher surface area of MCM-41 compared to Laponite, as well as to its more exposed SiO_4 tetrahedra. Nevertheless, and as measured by AAS, the amount of complex anchored in Laponite and in MCM-41 was similar (7.5 and 8 $\mu molg^{-1}$, respectively). This points out that, at least in the case of bulky complexes as the one used in this work, there is no clear benefit in using a material of high internal area regarding the total amount of complex anchored.

Activation of the amino-functionalized Laponite and MCM-41 by NaOEt create new surface nitrogen anionic species. This treatment resulted in an increase of the total amount of complex anchored for Laponite but, conversely, in a decrease in the case of the MCM-41 sample. In fact, in the case of the MCM-41 the treatment with NaOEt had a significant detrimental effect on the material porous structure, which may be related with the factors that affect the structural stability of this type of solids, as discussed elsewhere [59].

Acknowledgements This work was funded by Fundação para a Ciência e a Tecnologia (FCT) and FEDER, through the project ref. POCI/CTM/56192/2004. PD thanks FCT for a Post-Doctoral fellowship.

References

1. Jacobsen EN, Wu MH (1999) In: Pfaltz A, Jacobsen EN, Yamamoto H (eds) Comprehensive asymmetric catalysis. Springer-Verlag, Berlin
2. Katsuki T (1995) Coord Chem Rev 140:189
3. McGarrigle EM, Gilheany DG (2005) Chem Rev 105:1563
4. Choudary BM, Chowdari NS, Kantam ML, Santhi PL (2001) Catal Lett 76:213
5. Park DW, Choi SD, Choi SJ, Lee CY, Kim GJ (2002) Catal Lett 78:145
6. Piaggio P, Langham C, McMorn P, Bethell D, Bulman-Page PC, Hancock FE, Sly C, Hutchings GJ (2000) J Chem Soc Perkin Trans 2:143
7. Bigi F, Moroni L, Maggi R, Satori G (2002) Chem Commun 716:716
8. Kim GJ, Kim SH (1999) Catal Lett 57:139
9. Zhang HS, Xiang J, Xiao LC (2005) J Mol Catal A Chem 238:175
10. Kureshy RI, Ahmad I, Khan NH, Abdi SHR, Singh S, Pandia PH, Jasra RV (2005) J Catal 235:28
11. Xiang S, Zhang Y, Xin Q, Li C (2002) Chem Commun 2696
12. Xia Q-H, Ge H-Q, Ye C-P, Liu Z-M, Su K-X (2005) Chem Rev 105:1603
13. Zhang H, Xiang S, Li C (2005) Chem Commun 1209
14. Kim G-J, Shin J-H (1999) Tetrahedron Lett 40:6827
15. Sabater MJ, Corma A, Domenech A, Fornes V, Garcia H (1997) Chem Commun 1285
16. Heinrichs C, Holderich WF (1999) Catal Lett 58:75
17. Gbery G, Zsigmond A, Balkus KJ Jr (2001) Catal Lett 74:77
18. Reger TS, Jinda KD (2000) J Am Chem Soc 122:6929
19. Angelino MD, Laibinis PEJ (1999) Polym Sci A Polym Chem 37:3888
20. Song CE, Roh EJ, Yu BM, Chi DY, Kim SC, Lee KJ (2000) Chem Commun 615
21. Minutolo F, Pini D, Petri A, Salvadori P (1996) Tetrahedron Asym 7:2293
22. Canali L, Cowan E, Deleuze H, Gibson CL, Sherrington DC (2000) J Chem Soc Perkin Trans 2055
23. Kureshy RI, Khan NH, Abdi SHR, Ahmad I, Singh S, Jasra RV (2003) Catal Lett 91:207
24. Fraile JM, García JI, Massam JA, Mayoral JA (1998) J Mol Catal A Chem 136:47
25. Kureshy RI, Khan NH, Abdi SHR, Ahmad I, Singh S, Jasra RV (2004) J Catal 221:234
26. Silva AR, Vital J, Figueiredo JL, Freire C, Castro B (2003) New J Chem 27:1511
27. Silva AR, Castro B, Freire C (2004) Carbon 42:3027
28. Silva AR, Budarin V, Clark JH, Castro B, Freire C (2005) Carbon 43:2096
29. Baleizão C, Gigante B, Sabater MJ, Garcia H, Corma A (2002) Appl Catal A Gen 228:279
30. Shylesh S, Mirajkar SP, Singh AP (2005) J Mol Catal A Chem 239:57
31. Zhou XG, Yu XQ, Huang JS, Li SG, Li LS, Che CM (1999) Chem Commun 1789
32. Dioos BML, Geurts WA, Jacobs PA (2004) Catal Lett 97:125
33. Serrano DP, Aguado J, Garcia RA, Vargas C (2005) Stud Surf Sci Catal B 158:1493
34. Wheeler PA, Wang J, Baker J, Mathias LJ (2005) Chem Mater 17:3012
35. Herrera NN, Letoffe J-M, Reymond J-P, Bourgeat-Lami E (2005) J Mater Chem 15:863
36. Herrera NN, Letoffe J-M, Putaux JL, David L, Bourgeat-Lami E (2004) Langmuir 20:1564
37. Park M, Shim IK, Jung EY (2004) Phys Chem Solids 65:499
38. Biernacka IK, Silva AR, Carvalho AP, Pires J, Freire C (2005) Langmuir 21:10825
39. Pereira C, Patrício S, Silva AR, Magalhães AL, Carvalho AP, Pires J, Freire C (2007) J Colloid Interface Sci 316:570
40. Pereira C, Silva AR, Carvalho AP, Pires J, Freire C (2008) J Mol Catal A Chem 283:5
41. Jia M, Seifert A, Thiel WR (2003) Chem Mater 15:2174
42. Baleizão C, Gigante B, Garcia H, Corma A (2003) J Catal 5:99
43. Das P, Silva AR, Carvalho AP, Pires J, Freire C (2008) Colloids Surf A: Physicochem Eng Aspects 329:190
44. Das P, Silva AR, Carvalho AP, Pires J, Freire C (2009) Catal Lett (in press). doi:10.1007/s10562-008-9793-x
45. Grün M, Unger KK, Matsumoto A, Tsutsumi K (1997) In: McEnaney B, Mays TJ, Rouquerol J, Rodríguez-Reinoso F, Sing K, Unger KK (eds) Characterisation of porous solids IV. The Royal Society of Chemistry, London
46. Schmidt R, Stöcker M, Hansen E, Akporiaye D, Ellestad OH (1995) Microporous Mater 3:443
47. Rouquerol F, Rouquerol J, Sing K (1999) Adsorption by powders & porous solid. Academic Press, London
48. Benazilla M, Manne S, Laney DE, Lyubchenko YL, Hansma HG (1995) Langmuir 10:665
49. Tatsumi T (2005) Proceedings of 15th Saudi-Japan joint symposium, Dahram, Saudi Arabia
50. Handbook of chemistry and physics, 53rd edn. CRC Press, Boca Raton, 1972
51. Sing KSW, Everett DH, Haul RAW, Moscou L, Pierotti RA, Rouquerol J, Siemieniewska T (1985) Pure Appl Chem 57:603

52. Barret EP, Joyner LG, Halenda PP (1951) J Am Chem Soc 73:373
53. Lukens WJ Jr, Schmidt-Winkel P, Zhao D, Feng J, Stucky GD (1999) Langmuir 15:5403
54. Zhao XS, Lu GQ (1998) J Phys Chem B 102:1556
55. Gavrilko T, Gnatyuk I, Puchkovskaya G, Goltsov Y, Matkovskaya L, Baran J, Ratajczak H (2000) Vib Spectrosc 23:199
56. Borodko Y, Ager JWIII, Marti GE, Hong H, Niesz K, Somorjai GA (2005) J Phys Chem B 109:17386
57. Prado AGS, Airoldi C (2002) J Mater Chem 12:3823
58. Bourlinos AB, Simopoulos A, Boukos N, Petridis D (2001) J Phys Chem B 105:7432
59. Igarashi N, Koyano KA, Tanaka Y, Nakata S, Hashimoto K, Tatsumi T (2003) Microporous Mesoporous Mater 59:43